A Statistical Theory of Mobile-Radio Reception

By R. H. CLARKE

The statistical characteristics of the fields and signals in the reception of radio frequencies by a moving vehicle are deduced from a scattering propagation model. The model assumes that the field incident on the receiver antenna is composed of randomly phased azimuthal plane waves of arbitrary azimuth angles. Amplitude and phase distributions and spatial correlations of fields and signals are deduced, and a simple direct relationship is established between the signal amplitude spectrum and the product of the incident plane waves' angular distribution and the azimuthal antenna gain.

The coherence of two mobile-radio signals of different frequencies is shown to depend on the statistical distribution of the relative time delays in the arrival of the component waves, and the coherent bandwidth is shown to be the inverse of the spread in time delays.

Wherever possible theoretical predictions are compared with the experimental results. There is sufficient agreement to indicate the validity of the approach. Agreement improves if allowance is made for the nonstationary character of mobile-radio signals.

1. INTRODUCTION

In a typical mobile-radio situation one station is fixed in position while the other is moving, usually in such a way that the direct line between transmitter and receiver is obstructed by buildings. At ultra-high frequencies and above, therefore, the mode of propagation of the electromagnetic energy from transmitter to receiver will be largely by way of scattering, either by reflection from the flat sides of buildings or by diffraction around such buildings or other man-made or natural obstacles.

1.1 *The Model*

It therefore seems reasonable to suppose that at any point the received field is made up of a number of generally horizontally trav-

eling free-space plane waves whose azimuthal angles of arrival occur at random for different positions of the receiver, and whose phases are completely random such that the phase is rectangularly distributed throughout 0 to 2π. The phase and angle of arrival of each component wave will be assumed to be statistically independent. The probability density function $p(\alpha)$ which gives the probability $p(\alpha)d\alpha$ that a component plane wave will occur in the azimuthal sector from α to $\alpha + d\alpha$ will not be specified, since it will be different for different environments, and is also likely to vary from region to region within one environment; but the assumption that the phase φ has a rectangular probability density function throughout 0 to 2π will be made in all cases.

For simplicity, it will be assumed that at every point there are exactly N component waves and that these N waves have the same amplitude. In addition it will be assumed that the transmitted radiation is vertically polarized, that is, with the electric-field vector directed vertically, and that the polarization is unchanged on scattering so that the received field is also vertically polarized.

The model described so far gives what might be termed the "scattered field," since the energy arrives at the receiver by way of a number of indirect paths. Another term for this scattered field is the "incoherent field," because its phase is completely random. Sometimes a significant fraction of the total received energy arrives by way of the direct line-of-sight path from transmitter to receiver. The phase of the "direct wave" is nonrandom and it may therefore be described as a "coherent wave." It will be seen later that the field in a heavily built-up area such as New York City is entirely of the scattered type, whereas the field in a suburban area with the transmitter not more than a mile or two distant is often a combination of a scattered field with a direct wave.

1.2 *Comparison With Other Proposed Models*

J. F. Ossanna[1] was the first to attempt an explanation of the statistical character of the received mobile-radio signal in terms of a set of interfering waves. He was concerned with measurements taken in a suburban environment, and assumed that reflection occurred at the flat sides of houses and that the incident and reflected waves form an interference pattern through which the receiver moves. He then assumed that all orientations of the sides of houses are equally likely, and hence obtained spectra for the randomly fading signal with the

angle between the direction of vehicle motion and the direction to the transmitter as a parameter.

There is quite good agreement between Ossanna's theoretical spectra and those derived from measurements on several suburban streets situated within 2 miles of the transmitter. There is marked disagreement, however, at very low frequencies and at frequencies in the region of the sharp cut-off associated with the maximum Doppler frequency shift. At very low frequencies the spectral energy is always observed to be higher than that predicted by theory, whether Ossanna's or the one we use in this paper. The reason for this is that neither theoretical model takes into account the large-scale variations in total energy which result from the changing topography between transmitter and mobile receiver.

The basic difference between Ossanna's theoretical model and the model used here is that the former is essentially a *reflection* model whereas the latter is essentially a *scattering* model and so includes the former as a special case. An example of the limitations of the reflection model can be seen from the experimental spectra plotted in Ossanna's paper. The spectra are derived from signal-fading records made on several streets whose inclination to the transmitter direction ranged from 15 degrees to 84 degrees, and in each case there is evidence of a shelf which cuts off at twice the maximum Doppler frequency shift. Ignoring the higher harmonics generated in the detection process, the reflection model predicts a spectral cutoff which depends on the direction of the street with respect to the transmitter, ranging from the maximum Doppler frequency shift itself when the street is at right angles to the transmitter direction to twice that value when the street is in line with the transmitter.

With the scattering model, on the other hand, the angular distribution $p(\alpha)$ of scattered waves can be chosen to predict the existence of a spectral shelf out to twice the Doppler frequency shift for any street direction. Another feature of the reflection model which makes it rather inflexible is that for every randomly oriented reflected wave there exists a direct wave incident on the mobile receiver and carrying the same power. Thus the ratio of coherent to incoherent power in the received signal is fixed, whereas in the scattering model this ratio is arbitrary and may be adjusted according to the environment.

In his study of energy reception in mobile radio, E. N. Gilbert[2] examined several models of the scattering type and established a number of important relationships between them. One feature com-

mon to all of them, however, was the uniform distribution of waves in angle, although he briefly mentioned the effect of a single strong component arriving directly from the transmitter. The first model Gilbert considered was that of N waves arriving from fixed directions, equally spaced in angle. The phases of the waves were assumed to be independent and uniformly distributed throughout 0 to 2π; their amplitudes were assumed to be Rayleigh distributed and independent, but with the same variance. In a second model the angles of arrival were allowed to occur at random with equal probability for any direction; the phases were again completely random but the amplitudes were assumed to be constant. (This model is the same as the one we use in this paper, with the restriction that $p[\alpha] = [2\pi]^{-1}$.) A third model was an extension of the second to include the case of an arbitrary distribution of the amplitudes. Gilbert showed that the second and third models were equivalent to the first for sufficiently large N.

1.3 *Scope*

This paper shows that the scattering model can be used to predict the statistical characteristics of the signal received at the antenna terminals, hence at the output of a square-law or envelope detector, of the mobile receiving vehicle. These characteristics include the probability distributions of amplitude and phase, spatial correlations, amplitude spectra, and frequency correlations.

A simple relationship is established between the spectrum of the signal input and the product of the azimuthal power gain $g(\alpha)$ of the antenna and the probability distribution function $p(\alpha)$ of the angle of arrival of the component waves. This relationship will be particularly useful in analyzing mobile-radio systems with directional antennas on the mobile unit.

Other topics discussed are the use of space and frequency diversity, coherent bandwidth, and random frequency modulation. Some comments also are made on the nonstationary aspects of mobile-radio fields and on the consequent need for their characterization in terms which will be useful to the mobile-radio system designer. Wbenever possible the theory is discussed in tbe light of available experiments.

II. FIRST-ORDER STATISTICS OF THE FIELD

2.1 *Theory*

Under the assumption that the total field at any receiving point is vertically polarized and is composed of the superposition of N

waves, the n^{th} wave arriving at any angle α_n to the x axis (Fig. 1) with phase φ_n, the field components at point 0 (the zero phase reference point) are

$$E_z = E_0 \sum_{n=1}^{N} \exp\{j\varphi_n\} \tag{1}$$

$$H_x = -\frac{E_0}{\eta} \sum_{n=1}^{N} \sin \alpha_n \exp\{j\varphi_n\} \tag{2}$$

$$H_y = \frac{E_0}{\eta} \sum_{n=1}^{N} \cos \alpha_n \exp\{j\varphi_n\}. \tag{3}$$

In these equations E_0 is the common (real) amplitude of the N waves and η is the intrinsic impedance of free space. The time variation is understood to be of the form $\exp\{j\omega t\}$. Notice that E_z will be proportional to the signal input to the receiver when a vertical dipole antenna is used, and that E_z, H_x, and H_y will be proportional to the three inputs from a Pierce antenna system.[2]

The three field components E_z, H_x, and H_y are complex Gaussian random variables, to a good approximation, provided that N is sufficiently large. This is a consequence of the Central Limit Theorem and the assumption that the phases φ_n are independent of each other and of the angles of arrival α_n. Thus each field component has a real part and an imaginary part which are approximately zero-mean Gaussian random variables of equal variance, the approximation improving for larger N, and provided that the phases φ_n are rectangularly distributed throughout 0 to 2π. Appendix A shows that under the same assumptions the real and imaginary parts of each field component are uncorrelated; they are therefore approximately statistically independent.[3]

An important consequence of this is that the envelope of all three field components (hence of the signals at the terminals of a vertical

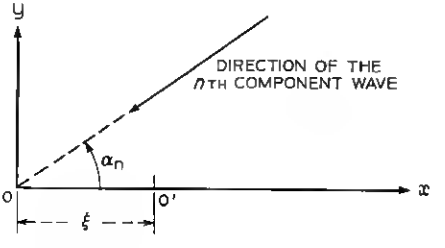

Fig. 1 — A typical component wave and the two field points 0 and 0'.

dipole antenna and of two orthogonal, vertical loops) will be Rayleigh distributed; and their phases will be rectangularly distributed throughout 0 to 2π. (See pp. 160–161 of Ref. 3.)

If, in addition to the N scattered waves, there is a wave of significant magnitude arriving directly from the transmitter, the resulting envelope and phase will no longer be respectively Rayleigh and rectangularly distributed. The relevant distributions will then be those derived by Rice[4] for a sine wave plus random noise. These distributions are, in general, quite complicated (see pp. 165–167 of Ref. 3), but in the limit, when the power in the direct wave is considerably greater than that in the combined scattered waves, both the phase and the envelope are approximately Gaussian distributed; the phase with zero mean and the envelope with a mean value equal to the amplitude of the direct wave.

2.2 *Experiment*

W. R. Young[5] has found that the Rayleigh distribution gives an excellent fit to the observed amplitude fluctuations in mobile-radio reception at 150, 450, 900, and 3700 MHz in New York City, provided that the sample area is less than about 1000 feet square. Trifonov, Budko, and Zutov, in a review of several investigations at 50, 150, and 300 MHz, also found that the Rayleigh distribution fits the data measured in rural suburbs at distances of about 5 and 9 km from the transmitter.[6] The fact that the measured distributions are Rayleigh in the above situations implies that there is no significant directly transmitted component and the fields are wholly of the scattered type, which seems physically reasonable.

Trifonov and his colleagues also found that for short transmission distances in towns (about 1 km), the signal amplitude has a nonzero-mean Gaussian distribution; and that for a transmission distance of 11 km in woodland, the signal has a Rice distribution. In these two cases there is apparently a significant direct component wave, and in the first case, where the transmission distance is only 1 km, the power in the direct component is considerably greater than that in the combined scattered components.

W. C. Jakes and D. O. Reudink have compared the statistical character of the amplitude of the fluctuating signal at the two frequencies of 836 MHz and 11200 MHz on the same street in a suburban environment at about 4 km from the transmitter. They find that the signal amplitudes are Rayleigh distributed at both frequencies, again

indicating that the direct wave is not significant.[7] This conclusion is borne out, for reasons discussed in Section 3.2.3, by the shape of the amplitude spectra which were computed from the same data.

The particular section of data which Jakes and Reudink analyzed was chosen with some care. The criterion of choice was that the data should "look" statistically uniform, and although this criterion is both arbitrary and subjective, it is important that it be applied in the absence of any other satisfactory criterion. The point is well illustrated by Fig. 2, which shows a section of signal-amplitude data at 836 MHz, obtained with a vertical dipole on a street adjacent to that used by Jakes and Reudink. The speed of the mobile receiver was 22 feet per second, and each of the five frames lasts about a second (time scale horizontal). The vertical scale is approximately linear in dB, covering a 70 dB spread with about 7 dB to each vertical division.

There is an obvious change in the statistics of the received signal in the fourth frame, compared with the others. (In fact, the fourth frame corresponds to the position of a street intersection, with one

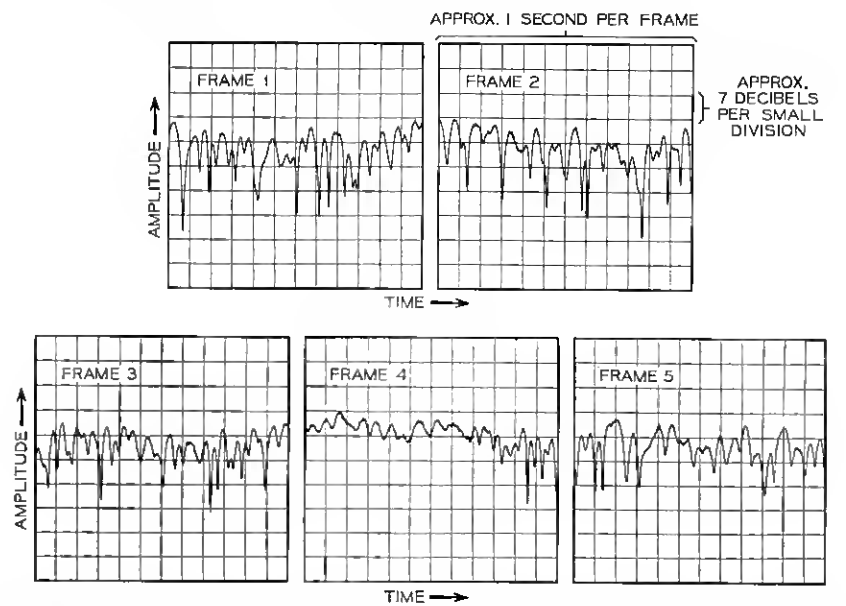

Fig. 2 — Section of a mobile radio data run, showing the variation of signal amplitude with time. (One vertical division is approximately 7 dB, and one horizontal frame is approximately 1 second.)

of the intersecting streets pointing in the direction of the transmitter. Then, according to the arguments used above, there will be a strong direct component which will raise the average signal level and change the distribution from a Rayleigh to a Rice or even a Gaussian. The average signal level in the fourth frame does rise, and the distribution does appear to be more symmetrical.) Using all five frames to estimate the probability density function would therefore be misleading in this case since obviously different parts of the data are samples of different distributions.

More subtle differences, as when the distributions underlying the data are all Rayleigh but with different variances over different parts of the run, can be equally misleading. Young found that whereas over fairly small areas of New York City the signal amplitude was accurately described by a Rayleigh distribution, over larger areas—even when the path of the receiver was roughly concentric with the transmitter—the data did not fit a Rayleigh distribution. This is examined in greater detail in Section VI.

III. SPATIAL CORRELATION OF FIELDS

3.1 *Theory*

The field components at some point 0 (see Fig. 1) in the mobile-radio field are given by equations (1), (2), and (3). At another point 0′, a distance ξ away from 0 in the x-direction, the phase of the n^{th} component wave will no longer by φ_n but $\varphi_n + k\xi \cos \alpha_n$, where $k = 2\pi/\lambda$ is the free-space phase constant. In the case of the electric field, the product of the complex conjugate of E_z (the field at 0) with E_z' (the field at 0′) is

$$\begin{aligned} E_z^* E_z' &= E_0^2 \sum_{n=1}^{N} \exp\{-j\varphi_n\} \sum_{n=1}^{N} \exp\{j(\varphi_n + k\xi \cos \alpha_n)\} \\ &= E_0^2 \sum_{n=1}^{N} \sum_{m=1}^{N} \exp\{j(\varphi_m - \varphi_n)\} \exp\{jk\xi \cos \alpha_m\}. \end{aligned} \tag{4}$$

Taking the average (that is, expectation) of both sides of equation (4), the autocovariance function of the electric field is

$$\begin{aligned} R_{E_z}(\xi) &= \langle E_z^* E_z' \rangle_{\text{av}} \\ &= E_0^2 \sum_{n=1}^{N} \sum_{m=1}^{N} \langle \exp\{j(\varphi_m - \varphi_n)\} \rangle_{\text{av}} \langle \exp\{jk\xi \cos \alpha_m\} \rangle_{\text{av}} . \end{aligned} \tag{5}$$

The angular parentheses denote "the average of" the quantity they enclose, and in this case may be thought of as an ensemble average

over all the possible situations implied by the assumed statistics of φ and α. The right-hand side is written as the product of two separate averages because of the statistical independence of φ and α. The first of these averages is zero except when $m = n$, so that

$$R_{E_z}(\xi) = E_0^2 \sum_{n=1}^{N} \langle \exp \{jk\xi \cos \alpha_n\} \rangle_{av} \tag{6}$$

$$= NE_0^2 \int_{-\pi}^{+\pi} p(\alpha) \exp \{jk\xi \cos \alpha\} \, d\alpha. \tag{7}$$

In the particular case when the N waves can arrive from any direction with equal probability,

$$p(\alpha) = \frac{1}{2\pi} \qquad -\pi \leqq \alpha \leqq +\pi, \tag{8}$$

the spatial autocovariance function of the electric field becomes

$$R_{E_z}(\xi) = \langle E_z^* E_z' \rangle_{av} = NE_0^2 J_0(k\xi). \tag{9}$$

The spatial autocovariance functions for the two components H_x and H_y of the magnetic field can similarly be shown to be

$$R_{H_x}(\xi) = \langle H_x^* H_x' \rangle_{av} = \frac{NE_0^2}{2\eta^2} [J_0(k\xi) + J_2(k\xi)] \tag{10}$$

and

$$R_{H_y}(\xi) = \langle H_y^* H_y' \rangle_{av} = \frac{NE_0^2}{2\eta^2} [J_0(k\xi) - J_2(k\xi)] \tag{11}$$

for waves arriving from any direction with equal probability. $J_0(\ )$ and $J_2(\ )$ are, respectively, the zero- and second-order Bessel functions of the first kind. The autocovariance functions (9), (10), and (11) are plotted in Fig. 3.

For the same probability density function $p(\alpha)$ of the equation (8) it can be shown in a similar manner that the cross-correlations of the field components are given by the following covariance functions.

$$R_{E_z H_x}(\xi) = \langle E_z^* H_x' \rangle_{av} = 0 \tag{12}$$

$$R_{E_z H_y}(\xi) = \langle E_z^* H_y' \rangle_{av} = j \frac{NE_0^2}{2y} J_1(k\xi) = -\langle E_z H_y'^* \rangle_{av} \tag{13}$$

$$R_{H_x H_y}(\xi) = \langle H_x^* H_y' \rangle_{av} = 0. \tag{14}$$

These equations show that all three field components are uncorrelated and therefore independent, since the fields are Gaussian at zero spatial

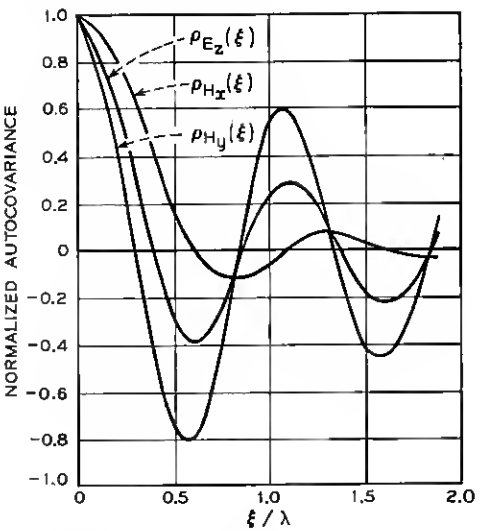

Fig. 3 — The normalized autocovariance functions $\rho_{E_z}(\xi)$, $\rho_{H_x}(\xi)$, and $\rho_{H_y}(\xi)$ from equations (9), (10) and (11).

separation. Further, E_z, H_x and H_x, H_y are uncorrelated and independent for all spatial separations, whereas E_z, H_y are correlated—except at spatial separations corresponding to the zeros of $J_1(\ )$, the first-order Bessel function of the first kind. The normalized covariance function for E_z and H_y is plotted in Fig. 4.

The autocovariance functions (9), (10), and (11) and the covariance functions (12), (13), and (14) are for the particular case of $p(\alpha)$ uniform in the interval $-\pi$ to $+\pi$. The autocovariance and covariance functions for any $p(\alpha)$ can be obtained from equation (7) and similar equations, but those derived here are useful illustrations as well as useful approximations in practice.

In any practical case, however, the complex field components E_z, H_x, and H_y cannot be measured. But their magnitude (that is, envelope or squared magnitude, that is, energy) can. Appendix B shows that the normalized autocovariance function of the departure from their mean of the squared magnitude of complex Gaussian random variables, such as the field components E_z, H_x, and H_y, is equal to the square of the normalized autocovariance function of the complex random variable itself. Taking the electric field E_z as an example, the normalized autocovariance function of the departure $\delta\,|E_z|^2$ of

the squared modulus from its mean is, from equation (9),

$$\rho_{\delta|E_z|^2}(\xi) = J_0^2(k\xi). \tag{15}$$

Similar normalized autocovariance functions and covariance functions for the squared magnitude of all three field components can be obtained from equations (10) through (14), and they can be shown to agree with the theoretical energy density correlations obtained by Gilbert.[2] This agreement was to be expected since energy density is derived from the squared magnitude of the field components; in addition, Gilbert used a theoretical model which is equivalent to that used here with uniform $p(\alpha)$.

With regard to the envelope of each of the complex field components, Appendix B also shows that the departure of the magnitude of such complex random variables from their mean is described by a normalized autocovariance function which is to a good approximation equal to the square of the normalized autocovariance function of the complex random variable itself. Thus, in the case of the electric field component E_z, again from equation (9),

$$\rho_{\delta|E_z|}(\xi) \cong J_0^2(k\xi). \tag{16}$$

(This quantity is also the normalized correlation coefficient of the signal envelopes at the terminals of two vertical monopole antennas ξ apart on the mobile receiving vehicle which is traveling through an isotropically scattered field.) Similar normalized autocovariance and covariance functions for the magnitudes of all three components can be obtained from equations (10) through (14).

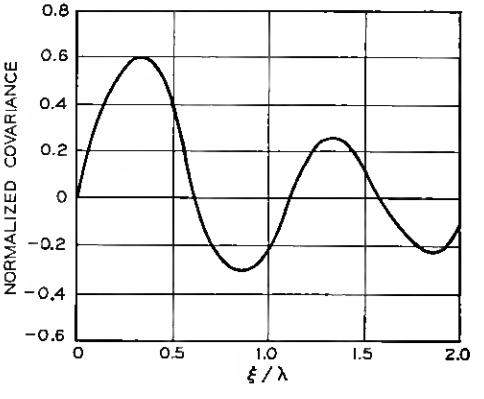

Fig. 4 — The normalized covariance function $\rho_{E_zH_y}(\xi)$, from equation (13).

3.2 *Experiment*

3.2.1 *Spatial Diversity*

Only indirect experimental evidence is available at this time on the spatial correlation of mobile-radio fields. In his measurements of the predetection combining of the signals from several equally spaced vertical monopole antennas, A. J. Rustako found that there was very little difference between the cumulative distributions of the combined amplitudes from four antennas spaced 1/4, 3/4, and 5/4 wavelengths apart.[8] Equation (16) indicates that the correlation coefficients of the signal amplitudes at the antenna terminals at these three separations are about 0.25, 0.06, and 0.03, respectively. Brennan has shown that such correlations produce very little difference in the combined signal from two channels,[9] and so the difference is presumably even less with four channels combined.

3.2.2 *Field Diversity*

Equations (12), (13), and (14) show that all three field components are uncorrelated (and therefore independent, because they are complex Gaussian random variables) at zero separation. The possibility of a "field diversity" system arising from this fact is exploited in the energy density reception scheme from Pierce.[2] (An alternate scheme, proposed by W. C. Jakes, would use predetection combining.[10] This has the advantage that the modulation is not affected.) W. C.-Y. Lee has devised and constructed an energy-density antenna[11] and his analysis of the measurements,[12] based on Gilbert's isotropic scattering model, show sufficient agreement with theory to indirectly confirm equations (12), (13), and (14) at $\xi = 0$.

3.2.3 *Frequency Spectra*

If the mobile receiving vehicle is moving with velocity V in the x direction, the spatial displacement ξ and the corresponding time displacement τ are related by

$$\xi = V\tau. \tag{17}$$

Then all the spatial correlations derived in Section 3.1 can be transformed into time correlations by using equation (17). The Fourier transform of the time autocovariance function then yields the frequency spectrum.

In the case of the signal at the terminals of a vertical monopole

antenna in an isotropically scattered field, equations (9) and (17) give the normalized time autocovariance function as

$$\rho_{E_z}(\tau) = J_0(kV\tau). \tag{18}$$

The corresponding input spectrum (see Ref. 3, p. 104) is given by

$$S_{E_z}(f) = \int_{-\infty}^{\infty} \rho_{E_z}(\tau) \exp(-j\omega\tau)\, d\tau \tag{19}$$

$$= \frac{1}{\pi f_m}[1 - f^2/f_m^2]^{-\frac{1}{2}} \qquad |f| \leqq f_m . \tag{20}$$

This spectrum is centered on the carrier frequency and is zero outside the limits $\pm f_m$ on either side of the carrier, where

$$f_m = \frac{V}{\lambda} \tag{21}$$

is the maximum Doppler frequency shift.

Gilbert[2] has shown that the corresponding baseband output spectrum from a perfect square-law detector is given by the complete elliptic integral,

$$S_{s|E_z|^2}(f) = \frac{1}{\pi^2 f_m} K\{[1 - (f/2f_m)^2]^{\frac{1}{2}}\}. \tag{22}$$

This output spectrum can be obtained either from the self-convolution of the input spectrum of equation (20) or by taking the Fourier transform of equation (15) expressed as a function of τ by means of equation (17). The spectrum of equation (22) also describes to good approximation the baseband output spectrum from an envelope detector (that is, half-wave linear rectifier). Thus,

$$S_{s|E_z|}(f) \cong \frac{1}{\pi^2 f_m} K\{[1 - (f/2f_m)^2]^{\frac{1}{2}}\}. \tag{23}$$

This is a consequence of the approximate equality of the spatial autocovariance functions of equations (15) and (16).

Figure 5 shows input and baseband output spectra for the above case of a vertical monopole antenna in an isotropically scattered field. The sharp cutoff in the baseband spectrum at twice the maximum Doppler shift is observed to some extent in all measured mobile-radio spectra.[1, 8] A small amount of spectral content will occur beyond this cutoff in the case of an envelope detector[13] because of the higher order terms neglected in the analysis, and in all cases because of the finite length of the time series used to compute the spectra. Again,

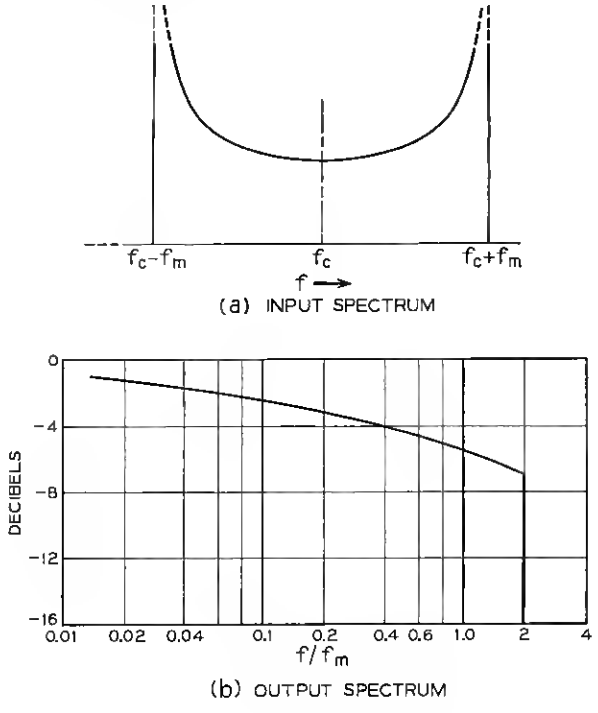

Fig. 5 — Input and baseband output spectra for a vertical monopole antenna in an isotropically scattered field.

in all cases the spectral content at the very low frequency end of the spectrum is much higher than that predicted by theory, owing to the nonstationary character of mobile-radio fields (see Section VI).

But in some cases, such as the spectrum obtained by Rustako,[8] there is reasonably good agreement between the general shape of the spectrum observed and that shown in Fig. 5b. Section IV shows that the theoretical spectra are different, except for the occurrence of the cutoff, if there is a significant directly transmitted component wave in addition to the scattered component waves. Most of the observed spectra seem to be of this latter type.

The above method of deriving spectra, by way of the Fourier transform of the autocovariance function, is not ideal. In all but the simplest cases (for example, when $p(\alpha)$ is uniform), direct integration of equation (7) is often impossibly difficult. As an alternative, the direct method (described in the next section) which depends on asso-

ciating a Doppler shift with the direction of arrival of each component wave, is much simpler to apply and allows one to retain a clear picture of the underlying physical processes.

IV. SIGNAL SPECTRUM AND ANGULAR PROBABILITY

There is a simple direct relationship between the signal spectrum at the mobile receiver's antenna terminals and the product $g(\alpha)p(\alpha)$. This is the product of the antenna's azimuthal power gain function $g(\alpha)$ and the probability density function $p(\alpha)$, the arrival angles of the plane waves which comprise the field incident on the antenna. Let us look at the use of the relationship for an omnidirectional antenna, the antenna assembly for the Pierce energy density scheme, and an azimuthally directive antenna.

4.1 *The General Relation*

The theoretical model proposed in Section 1.1 describes the field incident on the mobile receiving antenna in terms of a random set of vertically polarized plane waves incident horizontally which occur with probability density $p(\alpha)$, where α is the azimuth angle. Then, because of the vehicle's movement, each angle α (see Fig. 6) will be associated with a Doppler shift f in frequency from the carrier frequency, such that

$$f = f_m \cos \alpha$$

where

$$f_m = \frac{V}{\lambda} \tag{21}$$

is the maximum Doppler shift at the vehicle speed V and carrier wavelength λ.

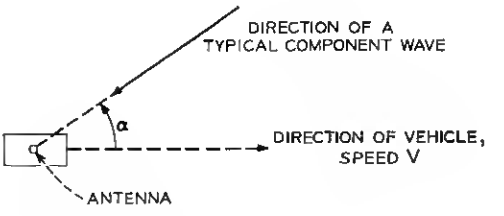

Fig. 6 — Relative directions of the mobile vehicle and a typical component plane wave.

Tbe spectrum of the signal v at the terminals of tbe receiving antenna on the mobile vehicle will consist of a set of spectral lines which will occur at random in the range $\pm f_m$ about the carrier frequency f_c. The probability that one of these spectral lines will occur in the range from f to $f + df$ is given by the probability density function $p_1(f)$, which may be obtained (see p. 33 of Ref. 3) from the probability density function $p(\alpha)$ by equating the differential probabilities

$$p_1(f)\,|df| = \{p(+\alpha) + p(-\alpha)\}\,|d\alpha| \tag{24}$$

since $+\alpha$ and $-\alpha$ give the same Doppler shift. Then, from equation (23),

$$p_1(f) = \frac{1}{f_m\sqrt{1 - f^2/f_m^2}} \cdot \{p(\alpha)\,|_{\alpha = \cos^{-1}(f/f_m)} + p(\alpha)\,|_{\alpha = -\cos^{-1}(f/f_m)}\}. \tag{25}$$

The signal spectrum $S_v(f)$, the average energy of the signal v in the frequency range f to $f + df$, is given by $p_1(f)$ weighted by the power gain $g(\alpha)$ of the antenna in the corresponding azimuthal direction α. Thus

$$S_v(f) = \frac{1}{f_m\sqrt{1 - f^2/f_m^2}} \cdot \{p(\alpha)g(\alpha)\,|_{\alpha = \cos^{-1}(f/f_m)} + p(\alpha)g(\alpha)\,|_{\alpha = -\cos^{-1}(f/f_m)}\} \tag{26}$$

which is the desired general relation. (See Appendix C for a formal proof.)

4.2 *Application of the General Relation*

4.2.1 *Omnidirectional Antennas*

The practical case of most frequent interest is that of a vertical monopole antenna, which has a constant azimuthal gain function, say $g(\alpha) = 1$. Assuming that $p(\alpha)$ is uniform for all angles throughout the range $-\pi$ to $+\pi$, $p(\alpha) = (2\pi)^{-1}$ and the signal spectrum at the antenna terminals would be

$$S_v(f) = \frac{1}{\pi f_m\sqrt{1 - f^2/f_m^2}} \tag{27}$$

for frequency shifts in the range $\pm f_m$ about the carrier frequency f_c, and would be zero outside that range. The spectrum of equation (27)

is identical to that of equation (20) which is for the electric field under the same circumstances, an identity that was to have been expected. The spectral shape of equation (27) is therefore that of Fig. 5a. The corresponding receiver baseband output spectrum, assuming square-law detection, would bo that of Fig. 5b.

The baseband output spectrum is considerably different if, in addition to the uniformly scattered set of waves, there is a significant wave transmitted directly from the transmitter to the receiver. If the angle of arrival of the direct wave is α_1 the spectrum of the signal at the terminals of an omnidirectional antenna would be that shown in Fig. 7a. This is the basic scattered spectrum of equation (27) together with a spectral line displaced from the carrier frequency by $f_m \cos \alpha_1$.

The corresponding output spectrum from a receiver with a square-law detector (or to good approximation if the detector is half-wave

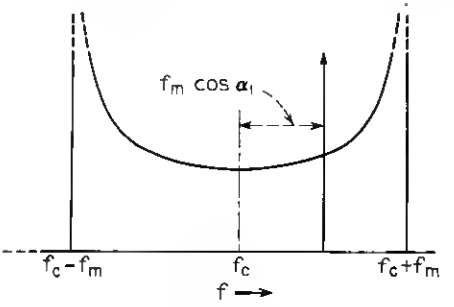

(a) INPUT SPECTRUM

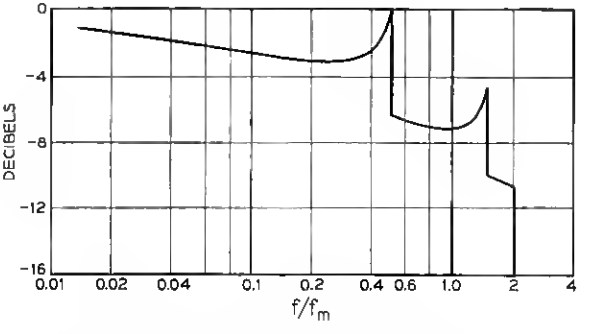

(b) OUTPUT SPECTRUM

Fig. 7 — Input and baseband output spectra for signals from an omnidirectional antenna, when a uniformly scattered field plus a direct wave are incident.

linear) may be obtained by convolving the above input spectrum with itself. (See p. 255 of Ref. 3.) This yields a baseband output spectrum of the form in Figure 7b, in which α_1 was chosen to be 60 degrees. In general, the high-frequency part of the baseband spectrum ends in a shelf which cuts off at twice the maximum Doppler frequency shift. (In the case of the half-wave linear detector there is a small amount of energy at frequencies beyond the cutoff frequency.)

There are two peaks in the baseband output spectrum which occur at $f = f_m(1 \pm \cos \alpha_1)$. Such peaks, as well as the final shelf, are clearly in evidence in Ossanna's experimental spectra.[1] Figure 8 shows two more experimental spectra, one where the direction to the transmitter was at right angles to the path of the receiving vehicle, and the other where the transmitter was directly ahead. The dashed curves are theoretical spectra with the ratio of power in the direct wave to the total scattered power adjusted arbitrarily. The theory apparently gives the basic form of the experimental spectra, but there are differences in detail.

Of course, complete agreement of theory and experiment is not to be expected. Apart from obvious changes, such as the speed of the vehicle and its inclination to the transmitter direction, the $p(\alpha)$ for the scattered waves and the magnitude of the direct wave will change throughout the entire data run. This means that the time series constituted by the output voltage of the receiver is not a stationary process, whereas the spectra are deduced on the assumption that it is. Methods of approaching this problem of the nonstationarity of mobile-radio data are discussed in Section VI, and methods of making a more valid comparison of theory and experiment are suggested.

4.2.2 *Vertical Loop Antennas*

As a simple example of an azimuthally directional antenna, the vertical loop is interesting because it forms part of the Pierce "total field" antenna system. (See Ref. 2, pp. 14 and 15, where this arrangement of a vertical monopole, together with two orthogonal vertical loops, is discussed in terms of the vertical component of the electric field and the two horizontal components of the magnitude field.)

Assume that the plane of loop 1 (see Fig. 9) lies in the direction of travel and that the plane of loop 2 lies perpendicular to that direction. Then the azimuthal power gain functions for the two orthogonal loops will be of the form

$$g_1(\alpha) = \cos^2 \alpha \tag{28}$$

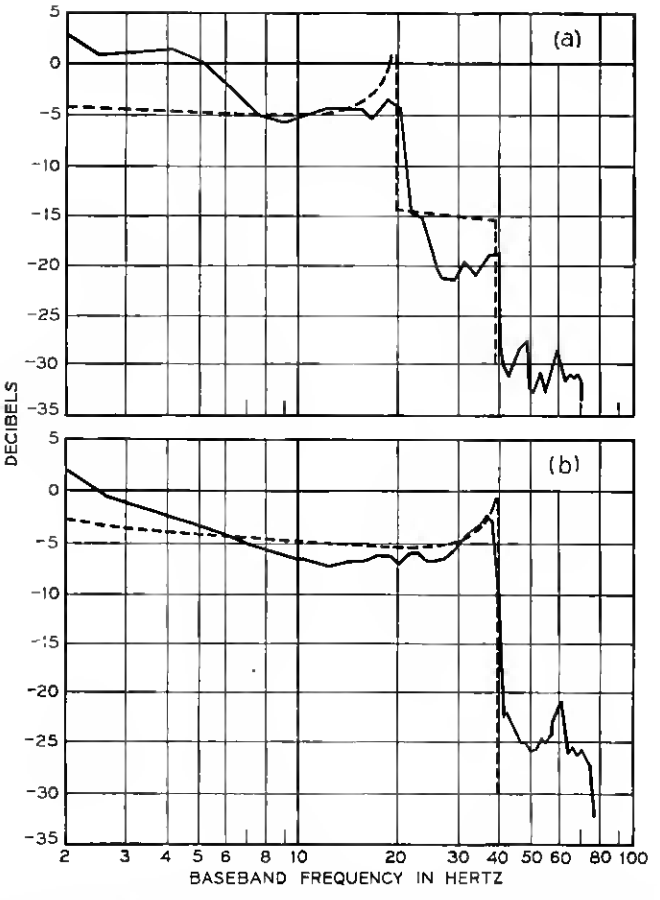

Fig. 8 — Comparison of theoretical (broken line) and experimental baseband output spectra with transmitter (a) at right angles to, and (b) directly ahead of, the vehicle patb.

and

$$g_2(\alpha) = \sin^2 \alpha, \tag{29}$$

respectively.

If it is further assumed that the scattered waves are uniformly distributed in angle, that is, $p(\alpha) = (2\pi)^{-1}$, and that there is no significant direct wave. Then, using the general relation of equation (26), the spectra of the signals at the terminals of the two loop

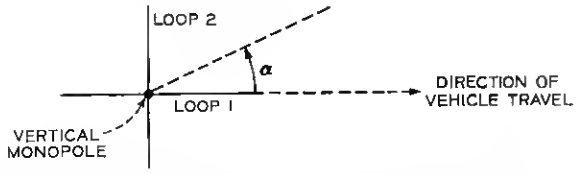

Fig. 9 — Plan view of Pierce antenna system, consisting of a vertical monopole and two orthogonal vertical loops.

antennas will be

$$S_1(f) = \frac{(f/f_m)^2}{\pi f_m \sqrt{1 - f^2/f_m^2}} \tag{30}$$

and

$$S_2(f) = \frac{\sqrt{1 - f^2/f_m^2}}{\pi f_m}. \tag{31}$$

Figure 10 shows these spectra with their corresponding baseband output spectra, assuming square-law detection in the receiver.

The spectra of equations (30) and (31) could also have been obtained from the autocovariance functions of equations (10) and (11) by substituting equation (17) and taking their Fourier transforms. However, the general relation is much simpler to use and indeed is the only reasonable method to use in cases where $p(\alpha)$ and $g(\alpha)$ are other than of the simplest functional form. In addition, the general relation preserves the physical description of the problem. Thus the shapes of the spectra in Fig. 10a have a straightforward explanation in terms of the antenna patterns emphasizing the Doppler shifts resulting from waves arriving from some directions and deemphasizing others—which is precisely the meaning of the general relation of equation (26).

4.2.3 *Beam Antennas*

The general relation of equation (26) gives a simple and direct solution for a beam antenna. The use of such highly directive antennas in mobile radio was suggested by W. C. Jakes[10] with a view to reducing the spectral width, and hence the rate of fading, of the received signal. The general relation shows immediately that such a reduction in spectral width does indeed occur, and gives the precise nature of that reduction.

Consider the idealized beam antenna pattern shown in Fig. 11. The power gain function $g(\alpha)$ in this case can be considered to be unity over the beamwidth β and zero in all other directions. If it is again assumed that the scattered waves are uniformly distributed in angle and that there is no significant direct wave, the effect of the antenna pattern on the spectrum of the signal at the antenna terminals can be thought of in terms of the pattern being a sectoral slice of a fictitious omnidirectional pattern. Hence the spectrum for the beam antenna is a slice taken from the spectrum for an omnidirectional pattern. See equation (27) and Fig. 5a.

When the beam antenna is directed broadside to the direction of

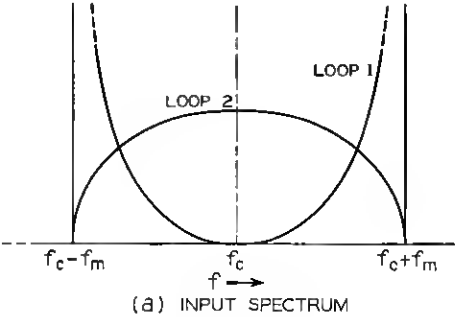

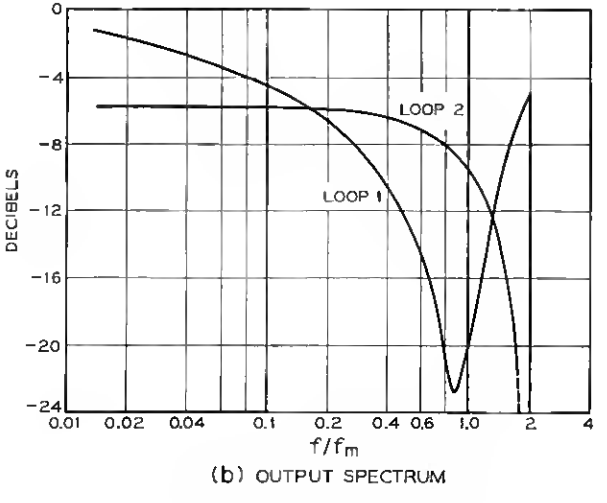

Fig. 10 — Receiver input and baseband output spectra for the two orthogonal loop antennas of Fig. 9.

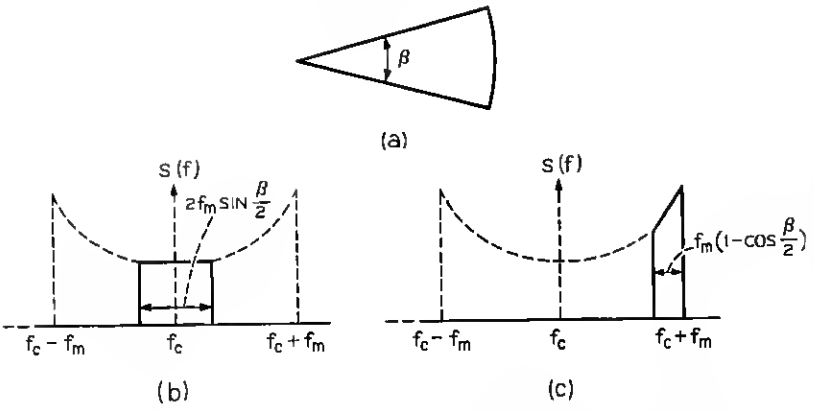

Fig. 11 — Receiver input spectra for an idealized beam antenna used in a uniformly scattered field. (a) Beam antenna pattern. (b) Spectrum for antenna directed broadside. (c) Spectrum for antenna directed straight ahead.

vehicle travel, the spectrum of the signal at the antenna terminals will be that shown in Fig. 11b, where the dashed curve shows the "remainder" of the omnidirectional spectrum. The spectrum is almost flat and is $2f_m \sin(\beta/2)$ wide.

When the beam antenna is pointed straight ahead, along the direction of vehicle travel, the spectrum is that shown in Fig. 11c. Instead of being centered on the carrier frequency, as in the broadside case, the spectrum occurs at the extreme right of the omnidirectional spectrum, and is $f_m[1 - \cos(\beta/2)]$ wide.

Thus it is apparent that the use of highly directive antennas in mobile radio will lead to a reduction in spectral width. W. C.-Y. Lee has confirmed this experimentally, using an array antenna at 836 MHz in a suburban environment.[14] Lee derived from the measured data the rate of crossing of the signal at a certain level and plotted this against antenna beamwidth. Rice has shown that for a narrow-band random signal which has a symmetrical spectrum about the carrier frequency, the rate of signal crossing at a certain level is just the probability density at that level multiplied by the square root of the second moment of the spectrum about the carrier frequency.[4] In this way the level crossing rate at a particular level is a measure of the width of the spectrum of the fading signal.

The sectoral beam pattern assumed in the early part of this section never occurs in practice. It is worth emphasizing this rather obvious point in connection with calculating spectral second moments. Because,

even though the antenna sidelobe level might be uniformly low, there will be spectral content throughout the entire range of $f_c \pm f_m$. Also, the basic omnidirectional spectrum emphasizes the contributions at the extremes of this range. Hence calculations of the spectral second moments might well be in error if they are based on the assumption that the side-lobe level is zero.

V. CORRELATION BETWEEN SIGNALS OF DIFFERENT FREQUENCIES

The problem of correlating two signals of slightly different frequencies occurs in mobile radio when questions of maximum usable bandwidth, or the use of a pilot signal at a frequency other than the carrier frequency, arise. Let us show that the covariance of two signals as a function of their frequency separation is simply the characteristic function of the probability density function of the time delays suffered by the component plane waves which are assumed to compose the mobile radio field.

5.1 *Theory*

Suppose that the transmitted signal contains two unmodulated signals of frequencies ω_1 and ω_2, whose difference $\Delta\omega = \omega_2 - \omega_1$ is small enough not to violate the following assumptions. Assume that the two signals take exactly the same time to travel from transmitter to mobile receiver along any one of the scattering paths assumed in the model in Section I. This assumption implies that propagation along all paths is by way of freespace type waves (which do not suffer dispersion), and that any phase changes experienced at reflecting or diffracting objects are independent of frequency. Associate a time of travel t_n with the n^{th} component wave, and define a time delay Δt in comparison with the shortest possible time of travel t_o such that

$$\Delta t_n = t_n - t_o . \tag{32}$$

To preserve the assumption made in all previous sections that the phases of the component waves are random and equally probable throughout 0 to 2π it is necessary that the average magnitude of the time delay difference between the n^{th} and m^{th} waves, assumed to be independent, be

$$\langle | t_n - t_m | \rangle_{\text{av}} \gg 1/f_c \tag{33}$$

where f_c is a frequency in the neighborhood of f_1 and f_2.

The electric fields at the two frequencies may be written as

$$E_1 = E_{01} \sum_{n=1}^{N} \exp \{j\omega_1(t - t_n)\}$$

$$E_2 = E_{02} \sum_{n=1}^{N} \exp \{j\omega_2(t - t_n)\}$$

where E_{01} is the amplitude at frequency f_1 of all the waves, and similarly E_{02} is the common amplitude at f_2. Forming the complex product

$$E_1^* E_2 = E_{01}^* E_{02} \exp \{j(\omega_2 - \omega_1)t\} \sum_{n=1}^{N} \sum_{m=1}^{N} \exp \{-j(\omega_2 t_m - \omega_1 t_n)\}$$

and taking the expectation of both sides,

$$\langle E_1^* E_2 \rangle_{av} = E_{01}^* E_{02} \exp \{j(\omega_2 - \omega_1)t\} \sum_{n=1}^{N} \langle \exp \{-j(\omega_2 - \omega_1)t_n\} \rangle_{av} \quad (34)$$

since it has been assumed that the time delays are independent, and therefore that

$$\langle \exp \{-j(\omega_2 t_m - \omega_1 t_n)\} \rangle_{av} = 0 \quad \text{for} \quad m \neq n$$

as a consequence of inequality (33). The covariance of the two fields as a function of their frequency separation $\Delta\omega$ is therefore

$$\begin{aligned} R_{12}(\Delta\omega) &= \langle E_1^* E_2 \rangle_{av} \\ &= N E_{01}^* E_{02} \exp \{j\,\Delta\omega t\} \exp \{-j\,\Delta\omega t_n\} \langle \exp \{-j\,\Delta\omega\,\Delta t\} \rangle_{av} \end{aligned}$$

where the subscript n has been dropped on Δt_n because the average is the same for any n. The normalized magnitude of $R_{12}(\Delta\omega)$ is:

$$| \rho_{12}(\Delta\omega) | = \langle \exp \{-j\,\Delta\omega\,\Delta t\} \rangle_{av} \quad (35)$$

is simply the characteristic function, with negative argument, of the probability density function for the time delays Δt. (See Ref. 3, p. 50.)

As an example, suppose that the time delays are exponentially distributed, so that the probability density function of Δt is

$$p(\Delta t) = \frac{1}{T} \exp \left\{ -\frac{\Delta t}{T} \right\} \quad \text{for} \quad 0 \leqq \Delta t \leqq +\infty \quad (36)$$

where T is a measure of the spread of the time delays. Then the normalized magnitude of the covariance function in equation (35) becomes

$$| \rho_{12}(\Delta\omega) | = [1 + (\Delta\omega T)^2]^{-\frac{1}{2}}, \quad (37)$$

which is shown in Fig. 12. It is apparent that the correlation falls off significantly for frequency separations $\Delta\omega > 1/T$, the inverse of the measure of the spread in time delays.

5.2 *Experiment*

Aside from its mathematical convenience, the exponential distribution of time delays seems physically plausible on the grounds that the shorter delays appear more likely to occur than the longer delays. Indeed, the pulse observations made by Young and Lacy at a frequency of 450 MHz in New York City support this contention.[15]

Ossanna has computed the envelope correlations from measurements at 860 MHz in a suburban environment for two-carrier frequency separations of 0.1, 0.5, 1.0, and 2.0 MHz.[16] The corresponding covariances are shown as circles in Fig. 12, where it has been assumed that $T = 1/4$ μsec. A comparison of these experimental points with the theoretical curve indicates that an exponential distribution of time delays is a reasonably good assumption, and that in the suburban environment where the experiments were performed the time-delay spread T is about $1/4$ μsec.

In contrast, Young and Lacy's pulse measurements indicate a time-delay spread about 5 μsec, but with an approximately exponential distribution. The reasons for the difference in time-delay spreads appears to result from the different environments in which the experiments were performed, not to the different frequencies, because their difference is not great. Thus in a suburban environment the component waves are likely to have been redirected by objects within a few hundred feet of the mobile receiver, whereas in New York City

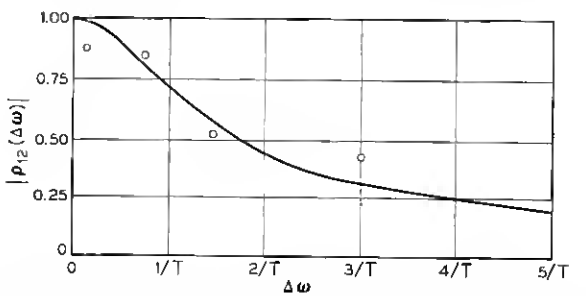

Fig. 12 — Normalized covariance of two signals as a function of their frequency separation, assuming an exponential distribution of time delays with delay spread T. The circles are Ossanna's experimental points.

the range of these objects can reasonably be put at many thousands of feet.

5.3 *Significance of the Random Time Delays*

The immediate benefit of knowing the probability distribution of the time delays of the component waves is that it enables one to deduce the "coherent bandwidth" for that particular system. But the significance of the time delays is much more than this, in that it emerges as a basic characteristic of the system along with the probability distribution of the angles of arrival of the component plane waves.

Indeed, it would appear that *a knowledge of the joint distribution* $p(\alpha,\Delta t)$ *of the angles of arrival* α *and the delay times* Δt *provides an almost complete description of the mobile radio field; hence, of the mobile radio signals sensed by antennas moving through this field.*

Thus, integration of the joint distribution with respect to α yields the distribution of time delays. Then if the standard deviation of the time delays is large compared with a period of the carrier frequency, the component waves may be said to be completely randomly phased and their phases and angles of arrival to be independent. The results obtained in Sections II, III, and IV would then follow, because they are based solely on the knowledge of $p(\alpha)$ and the assumptions that the phase is completely random and independent of the angle of arrival.

An interesting sidelight is that the cross-covariance of two signals of different frequencies, one shifted in time by τ from the other, depends on the joint distribution $p(\alpha, \Delta t)$. The Fourier transform of this cross-covariance yields the cross-spectrum of the two frequency-separated signals.

It is tempting to assume that α and Δt are independent, thus making the calculation much simpler. But this does not yield answers that accord with experiment; so one must conclude that α and Δt are not independent. This also seems a reasonable conclusion on physical grounds, since it is likely that the shortest time delays will be associated with angles of arrival from the general area of the transmitter, and that the longest delays will be associated with the opposite direction.

VI. THE NONSTATIONARY CHARACTER OF MOBILE RADIO SIGNALS

A perennial difficulty in the analysis of mobile-radio data is its nonstationary character. This makes both the analysis arbitrary and

its interpretation uncertain. This section attempts to meet this difficulty directly, rather than trying to find sections of data that "look" stationary or attempting to "doctor" data to that same end before it is analyzed.

The data chosen for analysis were those obtained by Rustako on a single omnidirectional antenna at 836 MHz along Sherwood Drive, a suburban street approximately 2 miles from the transmitter and running at an angle of about 48° to the transmitter direction.[8] The choice of data was made on the grounds that Rustako's computed output spectra most closely resembled the shape of the theoretical output spectrum of Fig. 5b which is for a completely scattered field with no significant directly transmitted component.

Two tests were performed on the data, one to determine the probability distribution of the envelope and the other to determine its time correlation by using Kolmogorov's structure function.

6.1 *The Probability Distribution*

6.1.1 *Theory for a Stationary Process*

According to the theory of Section 2.1, if the field incident on the mobile receiver is of the scattered type, each component wave being independent and randomly phased, then the probability density function (p.d.f.) of the envelope R is Rayleigh, that is,

$$p(R) = \frac{2R}{\sigma^2} \exp\left\{-\frac{R^2}{\sigma^2}\right\} \quad \text{for} \quad 0 \leqq R \leqq +\infty \tag{38}$$

which has the corresponding cumulative distribution function

$$P(R) = \int_0^R p(R)\, dR = 1 - \exp\left\{-\frac{R^2}{\sigma^2}\right\}. \tag{39}$$

This distribution has a root-mean-square value

$$\sqrt{R^2} = \sigma \tag{40}$$

a mean value

$$\langle R \rangle_{av} = \frac{\sqrt{\pi}}{2}\sigma = 0.886\sigma \tag{41}$$

and a most probable value (or "mode")

$$R\,|_{p\max} = \frac{1}{\sqrt{2}}\sigma = 0.707\sigma. \tag{42}$$

A convenient method of testing whether or not a given set of statistical data follow an assumed distribution is as follows.[17] First the histogram of the data (that is, relative frequency diagram), which is the practical approximation to the probability density function, is obtained. This is then summed point by point to give the cumulative frequency diagram, which is the practical approximation or estimate $\hat{P}(R)$ of the cumulative distribution function $P(R)$. Then $\hat{P}(R)$ is plotted against $P(R)$. If the two are identical for all R, then the resulting plot will be a straight line from (0, 0) to (1, 1). If not, the departure of the plot from the straight line is a measure of the departure of $\hat{P}(R)$ from $P(R)$.

In analyzing Rustako's data the question to be answered was how closely the data followed a Rayleigh distribution. The appropriate $P(R)$ is then that of equation (39); and the value of σ can be obtained from the maximum of the histogram with the aid of equation (42). The above arguments assume that the data is a stationary process.

6.1.2 *Theory for a Nonstationary Process*

If the theory of Section 2.1 is modified slightly to take account of the undoubted fact that either the number or the magnitude of the component waves will vary as the vehicle moves along its path by normalizing to the local mean, and if the assumption that the field is completely scattered is retained, then the expected distribution of the envelope will again be Rayleigh. However, the root-mean-square value σ will no longer be a constant, but will vary with time in some manner $\sigma(t)$. The envelope can now be classed as a nonstationary Rayleigh process.

It is possible to estimate $\sigma(t)$ from the record by computing the "local" mean $\langle R \rangle_{av}(t)$; then from equation (41)

$$\langle R \rangle_{av}(t) = 0.886\sigma(t). \tag{43}$$

Hence, writing the new random variable

$$r = \frac{R}{\sigma(t)} = \frac{0.886R}{\langle R \rangle_{av}(t)} \tag{44}$$

which in effect has a root-mean-square value of unity. The r process will be a stationary Rayleigh process with a p.d.f.

$$p(r) = 2r \exp \{-r^2\}.$$

Equations (43) and (44), in effect, remove the nonstationary effects

from the statistics. The meaning of "local" is explained further in the next section.

6.1.3 *Analysis*

Rustako's data, which had been converted to digital form at 500 samples per second, was taken in sets of 4000 points at a time. Notice that such a length of data contains approximately 200 fading cycles.

Each set was analyzed, first of all, on the assumption that it was stationary, by the method outlined in Section 6.1.1. To obtain the histogram, the amplitude range between the lowest and the highest value was divided into 50 equal slices. The $\hat{P}(R)$ versus $P(R)$ plots for three sets of data are shown on the left side of Fig. 13. Each point corresponding to a partiuclar slice level. The three sets of data were chosen to illustrate where $\hat{P}(R)$ is always greater than $P(R)$, where $\hat{P}(R)$ is always less than $P(R)$, and where they are approximately equal. On the assumption that all three sets of data are stationary it would have to be said that the first two cases are definitely non-Rayleigh while tho third case is.

Next, the same sets of data were normalized by the method outlined in Section 6.1.2. Tho local mean for every point was obtained by averaging the 200 points symmetrically adjacent to that point. The resulting normalized random variable was then treated in exactly the same way as the unnormalized random variable. The right side of Fig. 13 shows plots of $\hat{P}(r)$ versus $P(r)$. It can be seen that in the first two cases the normalized random variable is much more closely Rayleigh distributed than is the unnormalized random variable. The third case is interesting because, although the normalization was not necessary to reduce the data to a stationary Rayleigh process, it demonstrates that the technique of normalization itself does not significantly impair the original process.

In conclusion, it can be said that the technique of normalizing a nonstationary Rayleigh process by way of its running mean can be used to determine whether or not the process is in fact Rayleigh. But it must be emphasized that the technique cannot be applied to processes that are non-Rayleigh. It is certainly possible, however, that different techniques along these same lines might apply to different processes, although it would appear that some knowledge of the expected distribution is essential. The Rayleigh process is one of the simplest to handle because it is determined by a single parameter. In the example used here the Rayleigh process was clearly indicated

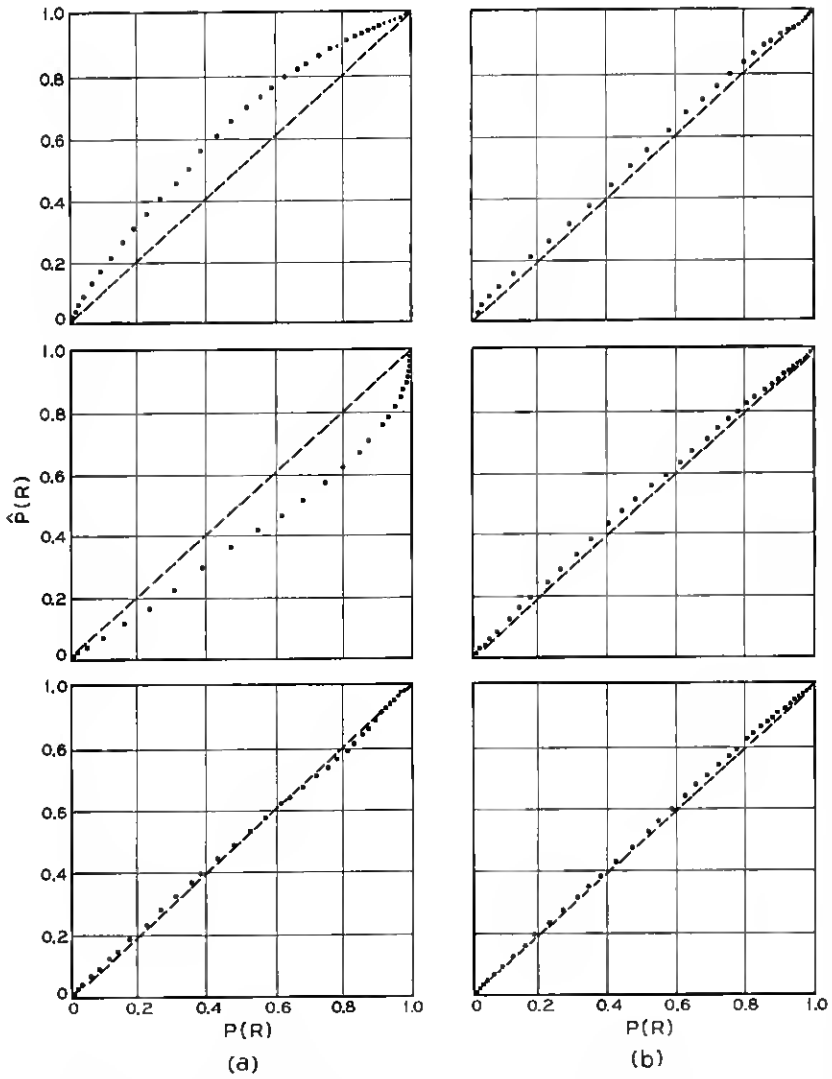

Fig. 13 — Plots of $\hat{P}(R)$ versus $P(R)$. (a) For the raw data. (b) For the same data normalized by its running mean.

by the theory, and the analysis amounts to a positive confirmation of its applicability.

6.2 *Using Kolmogorov's Structure Function*

Tartarski[18] has described the value of using a "structure function" in specifying random variables which are not statistically stationary. (The technique was first used by Kolmogorov to describe meteorological quantities.) The structure function might be of value in analyzing nonstationary mobile radio data.

6.2.1 *Definition and Properties*

The simplest type of structure function, $D_f(\tau)$ of the real random variable $f(t)$, is defined by

$$D_f(\tau) = \langle [f(t + \tau) - f(t)]^2 \rangle_{av} \tag{45}$$

where the angular parentheses denote a time average. This should be compared with the more commonly used autocovariance function, defined for a stationary random variable whose mean is zero by

$$R_f(\tau) = \langle f(t + \tau) f(t) \rangle_{av} . \tag{46}$$

Thus the structure function for a stationary random variable which can be written in terms of the autocovariance function is

$$D_f(\tau) = 2[R_f(0) - R_f(\tau)]. \tag{47}$$

As an example, the structure function for a stationary random variable with a Gaussian autocovariance function, $\exp \{-\tau^2/\tau_0^2\}$ in which τ_0 is constant, is depicted by the solid line in Fig. 14. The equation of this solid line is

$$D_f(\tau) = 2[1 - \exp \{-\tau^2/\tau_0^2\}].$$

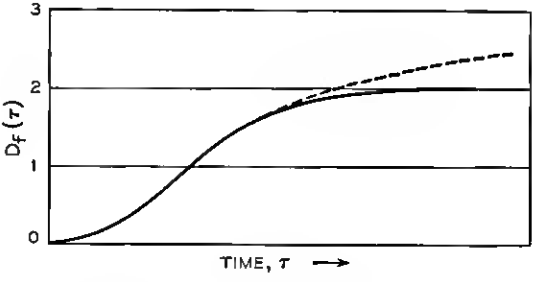

Fig. 14 — Structure functions for stationary (solid line) and nonstationary (dashed line) random variables.

Now, if the random variable is nonstationary in that it has, say, a slowly varying mean value, then the structure function would be modified in some way such as that shown dashed in Fig. 14. This dashed portion would very likely be indeterminate, so that the corresponding autocovariance function would be indeterminate *for all* τ. Hence the value of working, at least initially, with the structure function: if the random variable is stationary, that will immediately be apparent in that $D_f(\tau)$ will approach a horizontal asymptote for large τ; and if it is nonstationary, the portion for small τ can be relied on.

The dashed portion of Fig. 14 can be shown to correspond to an increase in low-frequency spectral energy compared with the stationary case.[18]

6.2.2 *A Structure Function Computed from the Data*

The solid line in Fig. 15 shows the structure function for Rustako's Sherwood Drive data, computed from the definition of equation (45). The data, again consisting of 4000 points, roughly straddled that which gave the first two probability plots of Fig. 13. The structure function is shown out to a time separation τ of 50 data points, or 100 msecs.

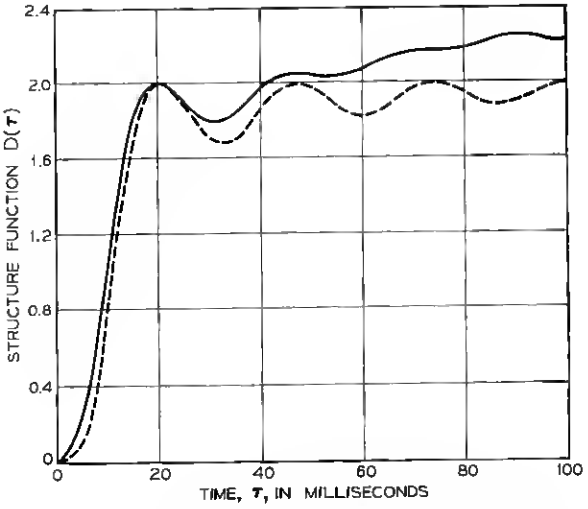

Fig. 15—Structure function computed for Rustako's data (solid line). The dashed line is the theoretical structure function for a stationary random variable.

The dashed curve is a theoretical structure function for an assumed stationary process with an auto-covariance function of the form $J_0^2(2\pi f_m \tau)$, where f_m is the maximum Doppler shift. This autocovariance function, which is derived from equations (16) and (17), is for the departure of the signal envelope from its mean value for the case of an omnidirectional antenna in a uniformly scattered field. The theoretical and experimental structure functions were arbitrarily made equal at the first maximum.

The experimental structure function, which is typical of many that were obtained, exhibits some of the features that were expected. The initial part of the curve, for small τ, closely follows the theoretical curve, and the quasiperiodic nature of the curve for large τ is also evident. In this region the experimental curve rises systematically above the theoretical curve, as was to be expected for nonstationary data.

This upward trend of the experimental structure function for large τ corresponds to the repeated observation of baseband low-frequency content at a significantly higher level than the theory predicts.

If this large-scale trend in the structure function were removed, then the modified structure function should agree with the theoretical structure function, provided that the basic assumptions of the theory are sound. The curves do differ, both in the amplitude and the period of the quasi-periodic variation. However, this might well result from the wrong choice of $p(\alpha)$, and not to a basic flaw in the theory.

It is evident that the structure function does afford a method of analyzing nonstationary data. The effect of large-scale variations shows up in the structure function and can be removed at that point, rather than by tampering in an arbitrary manner with the original data. Then the modified structure function can be compared with theoretical forms which are appropriate to stationary data.

VII. CONCLUSIONS

The theory presented in this paper attempts to explain the statistical behavior of fields and signals encountered in mobile radio in terms of a set of independent plane waves, redirected by scattering and reflecting obstacles, and incident horizontally on the mobile receiving vehicle. These waves can be described statistically by the joint probability density function $p(\alpha, \Delta t)$ such that the probability of a wave arriving at the azimuthal angle α with a time delay Δt is $p(\alpha, \Delta t) d\alpha d(\Delta t)$.

At ultrahigh frequencies and above, in urban and suburban environments, the spread in the magnitudes of the time delays is sufficiently large, compared with the radio-frequency period for the waves, to be considered randomly phased, in which case the following conclusions apply.

The field components are Gaussian, in the sense that their real and imaginary parts are independent zero-mean Gaussian random variables of equal variance. Thus the envelope of a signal derived from such a field by an antenna will be Rayleigh distributed, unless there is a significant nonscattered wave arriving directly from the transmitter, in which case the envelope will be Rice distributed.

The spatial correlation of the field components may be derived from the probability density function $p(\alpha)$. The spectrum of the signal at the antenna terminals may be derived from the product of $p(\alpha)$ with $g(\alpha)$, the azimuthal gain function of the antenna. The coherence of two radio frequencies, as a function of their frequency separation, may be derived from the probability density function of the time delays $p(\Delta t)$.

A brief examination of available experiments reveals that simple forms of both $p(\alpha)$ and $p(\Delta t)$ give theoretical results which agree broadly with experiment. We do not claim detailed agreement, nor does this seem possible until more complete experimental information is available. It does appear, however, that it is essential to take account of the nonstationary character of the signals obtained in mobile radio when attempting such a comparison.

The theoretical approach we have taken is midway between a purely phenomenological one, based on a complete catalog of the statistical characteristics of mobile-radio signals received under a variety of circumstances, and a purely analytical one in which the transmission environment is specified in detail. The phenomenological approach would be incomplete, in that it would not provide knowledge of why the signals have the character observed. The analytical approach is impossibly difficult to execute. Our approach, which seeks to describe the mobile-radio fields in terms of the compact (though not necessarily simple) quantity $p(\alpha, \Delta t)$, does provide the system designer with information which he can use to advantage in a straightforward way. The following is an example to illustrate this claim.

For example, suppose that experiments in a particular environment have shown that $p(\alpha)$ is roughly uniform and that $p(\Delta t)$ is approximately exponential with parameter T such that T is very large compared with the period of the proposed carrier frequency of

the mobile radio system. Then it is known that if an antenna with uniform gain in azimuth is used on the receiving vehicle the received signal will be a Rayleigh distributed fluctuating quantity with a baseband spectrum approximately uniform out to a frequency $2V/\lambda$, where V is the vehicle speed and λ is the carrier wavelength.

This system can be improved in a number of ways. The *depth* of fading, as Rustako has demonstrated,[8] can be reduced by using a number of such antennas separated by a sufficient distance for the signals to be essentially uncorrelated. The signals are then brought to a common phase, at which point they are combined before detection. The resulting signal is therefore the sum of a number of independent, Rayleigh distributed amplitudes, which for a large number will approach a Gaussian distribution with a nonzero mean.

Furthermore, the ratio of the root-mean-square fluctuation to the mean of the combined signal will decrease as the square root of the number of signals combined (by an approximate application of the Central Limit Theorem). Alternatively, the rate of fading, as Lee has demonstrated,[14] can be reduced by using directional antennas, which give a reduced spectral width of the fading* and hence a reduction in its rate.

W. C. Jakes has suggested a system, particularly suited for use at microwave frequencies, which combines the advantages of both a reduced depth and a reduced rate of fading.[10] The system consists of a number of directive antennas mounted on a single mobile unit and pointing in different azimuthal directions. If the signals from the different antennas are brought to a common phase and then combined before detection, the resulting signal will not only be considerably reduced in bandwidth compared with the case if an omnidirectional antenna had been used, but its depth of fading will also be reduced according to the square root of the number of antennas used. The widest coherent bandwidth that can be transmitted in the situation assumed is about T^{-1}.

VIII. ACKNOWLEDGMENTS

I wish to express my gratitude to W. C. Jakes, Jr., for his continued interest and helpful criticism throughout the work reported here, to C. C. Cutler, D. J. Hudson, M. J. Gans, E. N. Gilbert, H. L.

*In this connection, in a strictly literal sense "the medium is the message." If, as has been assumed, an unmodulated carrier is transmitted, then the received signal on a single omnidirectional antenna is both amplitude- and frequency-modulated (see Appendix D) because of the movement of the receiver through the scattering medium.

Schneider, and W. R. Young, Jr., for very useful discussion, to J. F. Ossanna, Jr., and A. J. Rustako, Jr., for generously supplying some of their data and calculations, and to Mrs. C. L. Beattie and Mrs. J. K. Reudink for invaluable assistance with the computations.

APPENDIX A

On the Correlation of the Real and Imaginary Parts of the Field Components

It is important to know the precise conditions under which the six real random variables comprising the real and imaginary parts of the three field components of equations (1), (2), and (3) are uncorrelated. Thus

$$E_z = E_0 \sum_{n=1}^{N} \cos \varphi_n + jE_0 \sum_{n=1}^{N} \sin \varphi_n$$

$$H_x = -\frac{E_0}{\eta} \sum_{n=1}^{N} \sin \alpha_n \cos \varphi_n - j\frac{E_0}{\eta} \sum_{n=1}^{N} \sin \alpha_n \sin \varphi_n$$

$$H_y = \frac{E_0}{\eta} \sum_{n=1}^{N} \cos \alpha_n \cos \varphi_n + j\frac{E_0}{\eta} \sum_{n=1}^{N} \cos \alpha_n \sin \varphi_n .$$

Denoting the real and imaginary parts of each field component by the superscripts (r) and (i), the correlation coefficient of the real and imaginary parts of the electric field, is

$$\langle E_z^{(r)} E_z^{(i)} \rangle_{\text{av}} = E_0^2 \sum_{n=1}^{N} \sum_{m=1}^{N} \langle \cos \varphi_n \sin \varphi_m \rangle_{\text{av}} = 0$$

since the φ_n's are independent and rectangularly distributed throughout 0 to 2π.

Similarly,

$$\langle H_x^{(r)} H_x^{(i)} \rangle_{\text{av}} = \frac{E_0^2}{\eta^2} \sum_{n=1}^{N} \sum_{m=1}^{N} \langle \sin \alpha_n \sin \alpha_m \cos \varphi_n \sin \varphi_m \rangle_{\text{av}} = 0$$

and

$$\langle H_y^{(r)} H_y^{(i)} \rangle_{\text{av}} = \frac{E_0^2}{\eta^2} \sum_{n=1}^{N} \sum_{m=1}^{N} \langle \cos \alpha_n \cos \alpha_m \cos \varphi_n \sin \varphi_m \rangle_{\text{av}} = 0$$

with the additional assumption that the φ_n's and α_n's are statistically independent. It can also be shown, based on the foregoing assump-

tions, that the correlation coefficient for any component real part and any component imaginary part is zero.

Notice that the above correlation coefficients are zero whatever the probability density function $p(\alpha)$ is of the α_n's. Where $p(\alpha)$ is important is in the correlation coefficients for the component real parts with each other and for the component imaginary parts with each other. For example,

$$\langle E_z^{(r)} H_x^{(r)} \rangle_{av} = -\frac{E_0^2}{\eta} \sum_{n=1}^{N} \sum_{m=1}^{N} \langle \sin \alpha_n \cos \varphi_n \cos \varphi_m \rangle_{av}$$

is zero if the further assumption is made that $p(\alpha)$ is rectangular throughout $-\pi$ to $+\pi$. Then the correlation coefficient is zero for any pair of component real parts and for any pair of component imaginary parts.

APPENDIX B

Correlation of Fields—Their Magnitudes and Squared Magnitudes

Section 2.1 and Appendix A show that under certain conditions the fields in mobile radio are "Gaussian fields," which means that a typical field component F (either an electric or magnetic component) may be represented by

$$F = x + jy$$

where x and y are real, independent, zero-mean Gaussian random variables of equal variance. Thus

$$\langle x \rangle_{av} = \langle y \rangle_{av} = 0$$

$$\langle x^2 \rangle_{av} = \langle y^2 \rangle_{av} = \sigma^2$$

and since both x and y are Gaussian distributed, their independence is implied by

$$\langle xy \rangle_{av} = 0.$$

The theory in the main text is concerned with finding the covariance $\langle F_1^* F_2 \rangle_{av}$ of two such Gaussian fields, where F_1 and F_2 may be two field components separated in space, in time, in frequency, or in all three. Thus

$$F_1 = x_1 + jy_1$$

$$F_2 = x_2 + jy_2$$

and

$$R_F = \langle F_1^* F_2 \rangle_{av} = \langle x_1 x_2 \rangle_{av} + \langle y_1 y_2 \rangle_{av} + j(\langle x_1 y_2 \rangle_{av} - \langle x_2 y_1 \rangle_{av}).$$

If, as is most often the case, all real parts are uncorrelated with all imaginary parts,

$$\langle x_1 y_2 \rangle_{av} = \langle x_2 y_1 \rangle_{av} = 0$$

and

$$R_F = \langle F_1^* F_2 \rangle_{av} = \langle F_1 F_2^* \rangle_{av} = \langle x_1 x_2 \rangle_{av} + \langle y_1 y_2 \rangle_{av} \tag{48}$$

is wholly real.

In practice it is not possible to measure the correlation of the complex fields. But what can be measured is the correlation of their magnitudes (that is, envelopes)

$$A = | F | = \sqrt{x^2 + y^2}$$

and the correlation of their squared magnitudes (that is, energies)

$$A^2 = | F |^2 = FF^* = x^2 + y^2.$$

The relation between the autocovariance functions R_F, R_A, and R_{A^2} is as follows.

Consider first the autocovariance function for squared magnitude

$$\begin{aligned} R_{A^2} = \langle | F_1 |^2 | F_2 |^2 \rangle_{av} &= \langle F_1 F_1^* F_2 F_2^* \rangle_{av} \\ &= \langle x_1^2 x_2^2 \rangle_{av} + \langle y_1^2 y_2^2 \rangle_{av} + \langle x_1^2 y_2^2 \rangle_{av} + \langle x_2^2 y_1^2 \rangle_{av} . \end{aligned}$$

To evaluate the right-hand side one may use the result that if $x_1, \ldots, x_4$ are real, zero-mean Gaussian random variables (see Ref. 3, p. 168),

$$\langle x_1 x_2 x_3 x_4 \rangle_{av} = \langle x_1 x_2 \rangle_{av} \langle x_3 x_4 \rangle_{av} + \langle x_1 x_3 \rangle_{av} \langle x_2 x_4 \rangle_{av} + \langle x_1 x_4 \rangle_{av} \langle x_2 x_3 \rangle_{av} .$$

Then, typically,

$$\langle x_1^2 x_2^2 \rangle_{av} = \langle x_1 x_1 x_2 x_2 \rangle_{av} = \sigma^4 + 2(\langle x_1 x_2 \rangle_{av})^2$$

and

$$\langle x_1^2 y_2^2 \rangle_{av} = \langle x_1 x_1 y_1 y_1 \rangle_{av} = \sigma^4$$

so that

$$R_{A^2} = 4\sigma^4 + 2[(\langle x_1 x_2 \rangle_{av})^2 + (\langle y_1 y_2 \rangle_{av})^2]. \tag{49}$$

Now, in most cases

$$\langle x_1 x_2 \rangle_{av} = \langle y_1 y_2 \rangle_{av} . \tag{50}$$

For example (48) and (50) can he shown to follow if F_1 and F_2 are the same field component, hut do not hold if F_1 is E_z and F_2 is H_z'.
Then equations (48) and (49) combined give

$$R_{A^2} = 4\sigma^4 + R_F^2, \tag{51}$$

or from equations (48) and (50)

$$R_{A^2} = 4\sigma^4(1 + \rho^2), \tag{52}$$

where ρ is the normalized autocovariance function of the x and y random processes.

The corresponding result for the autocovariance function of the magnitudes (see p. 59 of Ref. 13) is

$$\begin{aligned} R_A &= \langle A_1 A_2 \rangle_{av} = \langle |F_1| \, |F_2| \rangle_{av} \\ &= \sigma^2[2E(\rho) - (1 - \rho^2)K(\rho)], \end{aligned} \tag{53}$$

where K and E are the complete elliptic integrals of the first and second kind. In series form

$$R_A = \frac{\pi}{2}\sigma^2(1 + \rho^2/4 + \rho^4/64 + \cdots) \tag{54}$$

so that to a good approximation, neglecting powers of ρ higher than the second,

$$R_A \cong \frac{\pi}{2}\sigma^2(1 + \rho^2/4), \tag{55}$$

which has the same form as equation (52).

Finally, in terms of the field autocovariance function,

$$R_A \cong \frac{\pi}{2}\sigma^2\left(1 + \frac{R_F^2}{16\sigma^4}\right). \tag{56}$$

Both autocovariance functions R_{A^2} and R_A take on a much simpler form when normalized in the following way. Define the normalized autocovariance function of the departure δA^2 of the squared magnitude A^2 from its mean as

$$\rho_{\delta A^2} = \frac{\langle (A_1^2 - \overline{A_1^2})(A_2^2 - \overline{A_2^2}) \rangle_{av}}{\sqrt{\langle (A_1^2 - \overline{A_1^2})^2 \rangle_{av} \langle (A_2^2 - \overline{A_2^2})^2 \rangle_{av}}}. \tag{57}$$

Then from equation (52)

$$\rho_{\delta A^2} = \rho^2. \tag{58}$$

Defining the normalized autocovariance function of the departure δA of the magnitude A from its mean in a similar manner, equation (54) gives

$$\rho_{\delta A} = \frac{\pi}{4(4 - \pi)} (\rho^2 + \rho^4/16 + \rho^6/64 + \cdots), \tag{59}$$

or to a good approximation

$$\rho_{\delta A} \simeq \rho^2. \tag{60}$$

Equations (48) and (50) show that ρ is the normalized form of the autocovariance function R_F of the complex field component F.

APPENDIX C

Derivation of Equation 26

The complex amplitude of the received signal appearing at the antenna terminals may be written in the form

$$v = E_0 \sum_{n=0}^{N} a(\alpha_n) \exp \{j\varphi_n\}$$

where E_0 is the common amplitude of the N azimuthal plane waves incident on the mobile receiving antenna. The phase of each wave is φ_n, and $a(\alpha)$ is the voltage response at the antenna terminals owing to a unit-amplitude plane wave arriving at the azimuthal angle α. At another point a distance ξ away (see Fig. 1) the signal at the antenna terminals would be

$$v' = E_0 \sum_{m=1}^{N} a(\alpha_m) \exp \{j(\varphi_m + k\xi \cos \alpha_m)\}.$$

Forming the complex product v^*v' and taking its expected value to yield the spatial autocovariance function of the two signals, namely

$$R_v(\xi) = \langle v^*v' \rangle_{\text{av}}$$

$$= |E_0|^2 \sum_{n=1}^{N} \sum_{m=1}^{N} \langle a^*(\alpha_n)a(\alpha_m) \exp \{jk\xi \cos \alpha_m\} \rangle_{\text{av}} \cdot \langle \exp \{j(\varphi_m - \varphi_n)\} \rangle_{\text{av}}$$

where it has been assumed that the phases and angles of arrival of the component waves are independent. Making the further assumption that the phases are equiprobable throughout the range 0 to 2π,

$$R_v(\xi) = N |E_0|^2 \int_{-\pi}^{+\pi} p(\alpha)g(\alpha) \exp \{jk\xi \cos \alpha\} \, d\alpha \tag{61}$$

where $p(\alpha)$ is the probability density function of the component plane waves, and

$$g(\alpha) = a^*(\alpha)a(\alpha) = |a(\alpha)|^2$$

is the azimuthal power gain function of the antenna.

The temporal autocovariance function of v can be derived from equation (61) for a receiver moving with constant velocity V by making the substitution $\xi = V\tau$, where τ is a displacement in time. Then

$$R_v(\tau) = \int_{-\pi}^{+\pi} p(\alpha)g(\alpha) \exp \{j\omega_m\tau \cos \alpha\} \, d\alpha \tag{62}$$

where $\omega_m = 2\pi f_m$ with $f_m = V/\lambda$ the maximum Doppler shift, and $N |E_0|^2$ has been set equal to unity. The spectrum of the signal at the antenna terminals is given by the Fourier transform of the temporal autocovariance function of equation (62) and is

$$\begin{aligned} S_v(f) &= \int_{-\infty}^{\infty} R_v(\tau) \exp \{-j2\pi f\tau\} \, d\tau \\ &= \int_{-\infty}^{\infty} d\tau \int_{-\pi}^{+\pi} d\alpha p(\alpha)g(\alpha) \exp \{j(\omega_m \cos \alpha - 2\pi f)\tau\} \end{aligned} \tag{63}$$

where $f = \omega/2\pi$ is the shift in frequency from the carrier frequency.

Reversing the order of integration in equation (63), the integration w.r.t. τ yields a Dirac δ-function, thus

$$S_v(f) = \int_{-\pi}^{+\pi} p(\alpha)g(\alpha) \, \delta(f_m \cos \alpha - f) \, d\alpha. \tag{64}$$

Now writing

$$h(\alpha) = f_m \cos \alpha - f \tag{65}$$

it may be noticed that the δ-function of a function may be written in the form[19]

$$\delta[h(\alpha)] = \sum_n \frac{\delta(\alpha - \alpha_n)}{| h'(\alpha_n) |} \tag{66}$$

where the α_n are all the values of α for which $h(\alpha) = 0$, and the prime denotes differentiation w.r.t. α. Hence, from equations (64), (65), and (66) the spectrum of the signal at the antenna terminals is

$$S_v(f) = \frac{1}{f_m \sqrt{1 - f^2/f_m^2}} \cdot \{p(\alpha)g(\alpha) \, |_{\alpha = \cos^{-1}(f/f_m)} + p(\alpha)g(\alpha) \, |_{\alpha = -\cos^{-1}(f/f_m)}\}$$

which is equation (26). Notice that since the angle of arrival α must be real, the frequency sbift f must lie in the range $\pm f_m$.

APPENDIX D

Random Frequency Modulation of the Carrier

Since frequency modulation is often used in mobile radio systems it is pertinent to inquire what will be the nature of the received audio signal when a single unmodulated frequency is transmitted. The phase of the received signal is changing with time in a random manner; hence its instantaneous frequency is random.

It has been shown,[20] based on the work of Rice,[4] that the p.d.f. of the time-rate of change of phase θ' (the instantaneous frequency) for narrowband Gaussian random noise with an amplitude spectrum which is symmetrical about the carrier frequency, is

$$p(\theta') = \frac{1}{2}\left[\frac{b_2}{b_0}\left(1 + \frac{b_0}{b_2}\,\theta'^2\right)^3\right]^{-\frac{1}{2}} \tag{67}$$

where b_0 and b_2 are the zero$^{\text{th}}$ and second moments, respectively, about the carrier frequency of tbe amplitude spectrum $S(f)$. Notice that it has been assumed that there is no constant sinusoid present in the noise. It has also been shown[20] that the conditional p.d.f. $p(\theta'|r)$, which is the density of the instantaneous frequency given that the normalized envelope r is a certain value, is

$$p(\theta' \mid r) = \frac{1}{\sqrt{2\pi}\sigma'_\theta} \exp\left\{-\frac{\theta'^2}{2\sigma'^2_\theta}\right\} \tag{68}$$

which is a Gaussian distribution with zero mean and standard deviation

$$\sigma'_\theta = \frac{1}{r}\sqrt{\frac{b_2}{2b_0}}. \tag{69}$$

The above equations can be applied to the case of a mobile radio signal derived from an omnidirectional antenna in a uniformly scattered field.

The appropriate amplitude specturm is that of equation (27) and yields the moments,

$$b_0 = \int_{-\infty}^{\infty} S(f)\,df = 1 \tag{70}$$

and

$$b_2 = (2\pi)^2 \int_{-\infty}^{\infty} f^2 S(f)\, df = (1/2)\omega_m^2 \tag{71}$$

where ω_m is the maximum Doppler frequency shift in radians per second. Equations (67) and (68) then become

$$p(\theta') = \left[2\omega_m^2\left(1 + \frac{2\theta'^2}{\omega_m^2}\right)^3\right]^{-\frac{1}{2}} \tag{72}$$

and

$$p(\theta' \mid r) = \frac{1}{\sqrt{2\pi}\sigma'_\theta} \exp\left\{-\frac{\theta'^2}{2\sigma'^2_\theta}\right\} \tag{73}$$

with

$$\sigma'_\theta = (1/2)\frac{\omega_m}{r}. \tag{74}$$

The p.d.f. of equation (72) has a rather sharp maximum at $\theta' = 0$, and falls to about 0.2 of this maximum value at $\theta' = \pm\omega_m$. For large instantaneous frequency deviations the p.d.f. behaves asymptotically as the inverse cube of the frequency. In practical terms this p.d.f. is that of the amplitude of the output of a frequency discriminator in the receiver for a single frequency transmitted.

The conditional p.d.f. of equation (73), which is Gaussian in form, can also be interpreted as the p.d.f. of the amplitude of the discriminator output. But this is the p.d.f. of the frequency deviations measured only when the envelope amplitude is in the neighborhood of a particular level r, which is the envelope normalized by its r.m.s. value. In the particular example chosen the envelope has a Rayleigh distribution.

When $r = 1$ the conditional p.d.f. of the frequency deviations has a spread of the order of the maximum Doppler frequency shift ω_m. The spread will be 10 ω_m when $r = \frac{1}{10}$, the probability that $r \leqq \frac{1}{10}$ being 0.01. Similarly the spread will be 100 ω_m when $r = \frac{1}{100}$, the probability that $r \leqq \frac{1}{100}$ being 0.0001. Thus the wider ranges of random-frequency excursion are associated with only very small fractions of the total time.

REFERENCES

1. Ossanna, J. F., Jr., "A Model for Mobile Radio Fading Due to Building Reflections: Theoretical and Experimental Fading Waveform Power Spectra," B.S.T.J., *43*, No. 6 (November 1964), pp. 2935–2971.
2. Gilbert, E. N., "Energy Reception for Mobile Radio," B.S.T.J., *44*, No. 8 (October 1965), pp. 1779–1803.

3. Davenport, W. B. and Root, W. L., *An Introduction to the Theory of Random Signals and Noise*, New York: McGraw-Hill, 1958, p. 153.
4. Rice, S. O., "Statistical Properties of a Sine Wave Plus Random Noise," B.S.T.J., *27*, No. 1 (January 1948), pp. 109–157.
5. Young, W. R., Jr., "Comparison of Mobile Radio Transmission at 150, 450, 900, and 3700 Mc.," B.S.T.J., *31*, No. 6 (November 1952), pp. 1068–1085.
6. Trifonov, P. M., Budko, V. N., and Zotov, V. S., "Structure of USW Field-Strength Spatial Fluctuations in a City," (English translation from the Russian) Trans. Telecommunications Radio Eng., *9*, Pt. 1 (February 1964), pp. 26–30.
7. Jakes, W. C., Jr., and Reudink, D. O., "Comparison of Mobile Radio Transmission at UHF and X Band," IEEE Trans. Vehicular Technology, *VT-16* (October 1967), pp. 10–14.
8. Rustako, A. J., Jr., "Evaluation of a Mobile Radio Multiple Channel Diversity Receiver Using Pre-Detection Combining," IEEE Trans. Vehicular Technology, *VT-16* (October 1967), pp. 46–57.
9. Brennan, D. G., "Linear Diversity Combining Techniques," Proc. IRE, *47* (June 1959), pp. 1075–1102.
10. Jakes, W. C., Jr., unpublished work.
11. Lee, W. C.-Y., "Theoretical and Experimental Study of the Properties of the Signal from an Energy Density Mobile Radio Antenna," IEEE Trans. Vehicular Technology, *VT-16* (October 1967), pp. 25–32.
12. Lee, W. C.-Y., "Statistical Analysis of the Level Crossings and Duration of Fades of the Signal from an Energy Density Mobile Radio Antenna," B.S.T.J., *46*, No. 2 (February 1967), pp. 417–448.
13. Lawson, J. L. and Uhlenbeck, G. E., "Threshold Signals," Vol. 24 of MIT Radiation Laboratory Series, New York: McGraw-Hill, 1950, p. 63.
14. Lee, W. C.-Y., "Preliminary Investigation of Mobile Radio Signal Fading Using Directional Antennas on the Mobile Unit," IEEE Trans. Vehicular Comm., *VC-15* (October 1966), pp. 8–15.
15. Young, W. R., Jr. and Lacy, L. Y., "Echoes in Transmission at 450 Megacycles from Land-to-Car Radio Units," Proceedings of IRE, *38*, No. 3 (March 1950), pp. 255–258.
16. Ossanna, J. F., unpublished work.
17. Wilk, M. B., and Ghanadesikan, R., "Probability Plotting Methods for the Analysis of Data," Biometrika, *55*, part 1 (March 1968), pp. 1–19.
18. Tatarski, V. I., *Wave Propagation in a Turbulent Medium*, trans. R. A. Silverman, New York: McGraw-Hill, 1961, Chapter 1.
19. Zadeh, L. A. and Desoer, C. A., *Linear System Theory: The State Space Approach*, New York: McGraw-Hill, 1963, p. 533.
20. R.C.A., Defense Electronics Products, Surface Communications Systems Laboratory, final quarterly and summary report: *UNICOM Long Range Radio Circuits*, prepared under contract to Bell Telephone Laboratories, June 15, 1962.